AD-A188 599 SPECTROPHOTOMETRIC REMOTE SENSING OF THE DIFFUSE AURORA 1/1
(U) LOCKHEED MISSILES AND SPACE CO INC PALO ALTO CA
PALO ALTO RESEARCH LAB R R VONDRAK ET AL 30 NOV 87
UNCLASSIFIED LMSC/D868468 N00014-79-C-0824 F/G 4/1 NL

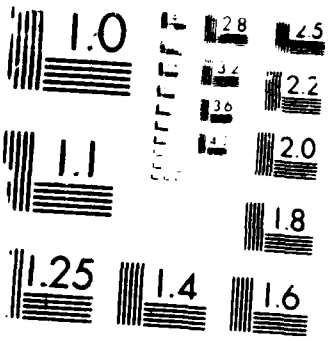
1.0
1.1
1.25
1.4
1.6
1.8
2.0
2.2
2.5
2.8
3.2
3.6

FINAL REPORT

For Period Ending 30 September 1987

ONR Contract N00014-79-C-0824

SPECTROPHOTOMETRIC REMOTE SENSING OF THE DIFFUSE AURORA

30 November 1987

R. R. Vondrak, Principal Investigator

Space Sciences Laboratory, D91-20, B255

Lockheed Palo Alto Research Laboratories

Prepared for:

Office of Naval Research
800 North Quincy Street
Arlington, Virginia 22217

SECURITY CLASSIFICATION OF THIS PAGE

REPORT DOCUMENTATION PAGE

Form Approved OMB No. 0704-0188

A188699

1a. REPORT SECURITY CLASSIFICATION
UNCLASSIFIED

1b. RESTRICTIVE MARKINGS

2a. SECURITY CLASSIFICATION AUTHORITY

3. DISTRIBUTION/AVAILABILITY OF REPORT
UNLIMITED. CLEARED FOR PUBLIC RELEASE AND SALE.

2b. DECLASSIFICATION/DOWNGRADING SCHEDULE

4. PERFORMING ORGANIZATION REPORT NUMBER(S)
LMSC/D068460

5. MONITORING ORGANIZATION REPORT NUMBER(S)

6a. NAME OF PERFORMING ORGANIZATION
LOCKHEED PALO ALTO RESEARCH LABORATORY

6b. OFFICE SYMBOL (If applicable)

7a. NAME OF MONITORING ORGANIZATION
OFFICE OF NAVAL RESEARCH
DEPARTMENT OF THE NAVY

6c. ADDRESS (City, State, and ZIP Code)
3251 HANOVER ST. B/255
PALO ALTO, CA. 94304

7b. ADDRESS (City, State, and ZIP Code)
800 NORTH QUINCY ST.
ARLINGTON, VIRGINIA 22217-5000

8a. NAME OF FUNDING/SPONSORING ORGANIZATION
AIR FORCE GEOPHYSICS LAB.

8b. OFFICE SYMBOL (If applicable)

9. PROCUREMENT INSTRUMENT IDENTIFICATION NUMBER
CONTRACT N00014-79-C-0824

8c. ADDRESS (City, State, and ZIP Code)
HANSCOM AFB. MA 01731

10. SOURCE OF FUNDING NUMBERS

PROGRAM ELEMENT NO	PROJECT NO	TASK NO	WORK UNIT ACCESSION NO

11. TITLE (Include Security Classification)
SPECTROPHOTOMETRIC REMOTE SENSING OF THE DIFFUSE AURORA

12. PERSONAL AUTHOR(S)
R. R. VONDRAK AND R. M. ROBINSON

13a. TYPE OF REPORT	13b. TIME COVERED	14. DATE OF REPORT (Year, Month, Day)	15. PAGE COUNT
FINAL REPORT	FROM 1 AUG. 79 TO 30 NOV 87	1987, NOVEMBER 30	

16. SUPPLEMENTARY NOTATION

17. COSATI CODES		
FIELD	GROUP	SUB-GROUP

18. SUBJECT TERMS (Continue on reverse if necessary and identify by block number)
ELECTRON PRECIPITATION
X-RAYS
REMOTE SENSING

19. ABSTRACT (Continue on reverse if necessary and identify by block number)

Auroral electron precipitation produces both E-region ionization and bremsstrahlung X-rays. In a set of coordinated observations these atmospheric effects of electron precipitation were measured simultaneously by the X-ray sensor on the DMSP/F2 spacecraft and by the incoherent-scatter radar at Chatanika, Alaska. In all data sets there was good agreement between the locations of the X-ray source regions and the regions of enhanced E-region ionization. Detailed comparisons were made between the measured and inferred altitude profiles of ionization for two auroral conditions, a premidnight auroral band and a sunlit diffuse aurora. These comparisons validate the ability to infer auroral ionization from satellite-based X-ray measurements.

20. DISTRIBUTION/AVAILABILITY OF ABSTRACT
☐ UNCLASSIFIED/UNLIMITED ☒ SAME AS RPT ☐ DTIC USERS

21. ABSTRACT SECURITY CLASSIFICATION
UNCLASSIFIED

22a. NAME OF RESPONSIBLE INDIVIDUAL

22b. TELEPHONE (Include Area Code)

22c. OFFICE SYMBOL

DD Form 1473, JUN 86 Previous editions are obsolete.

SECURITY CLASSIFICATION OF THIS PAGE

INTRODUCTION

Ionization in the earth's atmosphere is produced primarily by solar illumination and incoming energetic particles. Ionization produced by solar illumination is well understood and can be accurately modeled. But at high latitudes, particularly at night, the dominant source of ionization may be precipitating protons and electrons with energies less than about 100 keV. This makes modeling high latitude ionization difficult because these particle fluxes may be temporally and spatially varying. Global specification of the distribution of ionization at high latitudes is best done using detectors on space-based platforms capable of viewing a large portion of the earth at one time. This method involves detecting electromagnetic radiation originating from the impact of charged particles into the atmosphere. This radiation may be in the X-ray, ultraviolet, or visible portion of the spectrum. The X-ray and ultraviolet techniques hold great promise for remotely sensing ionization because of the absence of a background emission source that prohibits imaging of aurorally-produced emissions in the sunlit hemisphere. However, detailed comparisons between modeled and measured auroral emissions are required to assess the accuracy of these techniques.

In this study we compare simultaneous measurements by the Chatanika radar and the DMSP-F2 satellite X-ray detector to demonstrate that remote X-ray observations can be used to infer the ionization produced by diffuse auroral electron precipitation. Globally, diffuse auroral electron precipitation accounts for the bulk of the energy deposited in Earth's atmosphere by precipitating particles. Thus, it is important to validate remote sensing techniques using emissions produced by this type of aurora. In this study, the accuracy of the X-ray remote sensing is assessed by a quantitative comparison between the profiles of ionization measured by the ground-based incoherent-scatter radar and the profiles inferred from the satellite-based X-ray measurements. Measurements were made in two types of diffuse aurora: a dynamic evening diffuse aurora and a sunlit diffuse aurora in the morning sector.

The work described herein was performed under support from the Air Force Geophysics Laboratory in collaboration with Drs. P. F. Mizera and D. J. Gorney of the Aerospace Corporation who provided the DMSP X-ray data. The results of this study have been reported by Vondrak et al. (1987).

INFERENCE OF AURORAL ELECTRON FLUXES FROM X-RAYS

Precipitating electrons interact with the atmosphere to produce ionization and various forms of electromagnetic radiation. Excitation of neutral and ionic constituents caused by impact of primary and secondary electrons leads to optical emissions at virtually all wavelengths. In addition, the slowing down of the primary electrons produces bremsstrahlung X-ray emission. The inference of ionization produced by the precipitating electrons is done by determining their spectral distribution from the measured emissions. Because we are here restricting our discussion to altitudes between 80 and 200 km, the electron energy range of interest is approximately 500 eV to 100 keV. Once the electron spectral distribution is known, the resulting ionization can be accurately modeled (see, for example, Vondrak and Robinson, 1985). Thus, remote sensing depends on the accuracy with which the energy distribution of the precipitating electrons can be determined from the measured emissions.

The flux of X-rays F_x of energy E_x is given by

$$F_x(E_x) = \int_{E_x}^{\infty} \Phi(E_x, E_e) F_e(E_e) dE_e \qquad (1)$$

where F_e is the flux of electrons of energy E_e. The function $\Phi(E_x, E_e)$ is a source function relating the two fluxes. In this expression, absorption of X-rays in the atmosphere is neglected; this is justified for most auroral electron spectra where the average energy of the electrons is well below about 40 keV. Determination of the electron fluxes from the measured X-ray fluxes involves deconvolution of this integral equation. There have been several approaches to this problem. For the experiments described below we use the inversion technique described by Brown (1972). Errors may arise in the inversion procedure, particularly at low electron energies, because for typical auroral electron spectra most of the low energy X-rays are produced by higher energy electrons. Small errors in the measurement of the high energy X-ray flux can thus translate to large errors in the low energy electron flux. Fortunately, however, electrons with energies below a few keV are relatively inefficient at producing E region ionization, so that the electron density profiles determined from the inferred electron spectra are fairly well reproduced.

DESCRIPTION OF EXPERIMENTS

The ground-based ionization measurements were made with the Chatanika incoherent-scatter radar (Leadabrand et al., 1972; Baron, 1977; Vondrak, 1983). For these experiments the radar was generally operated in a variety of modes consisting of combinations of elevation scans and of fixed-position measurements. The ionization was measured with a range resolution of 4.5 km and with integration times of about 15 sec. Because the satellite and radar measurements are generally not spatially coincident nor simultaneous, ground-based all-sky photographs were used when possible to relate the measurements during the nighttime passes. Visible auroral imagery from the DMSP-F2 satellite was not available for the cases used in this study.

X-ray measurements were made with an auroral X-ray sensor on the DMSP-F2 satellite (Mizera et al., 1978). DMSP-F2 is in a nearly sun-synchronous circular polar orbit at an altitude of 830 km. The sensor field of view is 2° by 14°, providing an in-track spatial resolution of about 50 km and a cross-track resolution of about 350 km. This corresponds to about 0.5° of latitude by about 0.5 hour of local time. The downlooking X-ray sensor provides integral X-ray measurements in fifteen energy channels from 1.4 to 20 keV. These X-ray spectra were converted to equivalent incident electron spectra using the inversion technique described by Brown (1972). From these electron spectra we calculated the ionization production rate q as a funciton of altitude using the method of Rees (1963). The electron density n, was calculated assuming the model effective recombination coefficient α given by Vickrey et al. (1982). A transport-free equilibrium solution was used for the electron continuity equation, such that the electron density as a function of altitude z is given by

$$n(z) = \left[\frac{q(z)}{\alpha(z)}\right]^{\frac{1}{2}} \tag{2}$$

For the sunlit cases the production rate due to electron precipitation was added to the solar photoionization rate specified in the empirical model of Robinson and Vondrak (1984).

Precipitating electron fluxes in eight differential energy channels from 1-20 keV were measured once per second by the J/3 instrument on DMSP. Whenever available, the precipitating electron data were used as an independent test of the validity of the X-ray spectral inversion technique (see also, Mizera and Gorney, 1982).

The entire set of simultaneous Chatanika/DMSP-F2 observations was searched for cases that satisfy the criteria of spatial and temporal coincidence, with aurora present

within the Chatanika field-of-view. Another constraint was that the auroral luminosity and ionization had to be fairly homogenous over the X-ray sensor field of view. Only four cases were identified that met these criteria. In all cases there was good spatial coincidence between the regions of enhanced X-ray luminosity and the regions of enhanced ionization. During two cases the conditions of simultaneity and homogeneity were sufficiently good to allow a detailed quantitative comparison between the measured and inferred altitude profiles of ionization. In the next section we present in detail the observations made on these two days that are representative of auroral conditions in the evening sector and in the morning sunlit sector.

OBSERVATIONS OF AN EVENING AURORA

On 21 February 1979 the DMSP-F2 satellite passed slightly to the east of Chatanika at 0727 UT (2127 local time). The location of the satellite ground track is shown in Figure 1. During that night the Chatanika radar was operated in alternating elevation scans and fixed-position measurements. The E-region limits of the elevation scan closest in time to the satellite pass is shown in Figure 1.

During the DMSP pass there were bright auroral bands south and overhead of Chatanika. During the satellite pass the radar was pointed in several fixed positions within the auroral band. Following the satellite pass, the bright auroral bands moved southward. The Chatanika elevation scan began in the south within the bright auroral band. All-sky camera photographs taken at that time showed that the auroral band extended over the southern sky from the northwest to the southeast as shown by the shaded region in Figure 1. On the figure are shown the times corresponding to the beginning and end of the radar elevation scan. As the radar scanned northward the auroral conditions changed dramatically with the sudden appearance of rayed arcs and reduced auroral luminosity. These temporal variations were evident both in the all-sky photographs and in the Chatanika measurements made in the fixed-position mode and during the elevation scan. The radar ionization measurements during the elevation scan closest in time to the satellite pass are shown in Figure 2. The contours show electron density as a function of altitude and invariant latitude in the magnetic meridian plane. Conspicuous features are the enhanced ionization between 62° and 66° latitude that is associated with the bright visible auroral band, and the high-altitude ionization in the north between 66.6° and 67.2°. This latter ionization is associated with the rayed arcs that appeared after the satellite pass. The

peak E-region electron density in the bright auroral band varied between $3 \times 10^5 cm^{-3}$ and $6 \times 10^5 cm^{-3}$ and was situated at altitudes between 110 and 120 km. Electron densities in the rayed arcs maximized at altitudes near 140 km.

The X-ray sensor on the DMSP satellite detected enhanced X-ray fluxes at the latitudes near Chatanika. Because of the temporal variations in the aurora after the satellite pass, we compare the radar and satellite measurements made in the bright auroral band to the south of Chatanika which remained relatively stable. The energy distribution of bremsstrahlung X-rays in the auroral band south of Chatanika is shown in the first panel of Figure 3. Because of the large field of view of the X-ray sensor, this distribution represents a spatial average of the X-ray fluxes produced in the band.

The precipitating electron energy distribution inferred from the X-ray distribution in the auroral band is shown in the middle panel of Figure 3. For comparison we show in Figure 3 the direct measurement of the precipitating electron flux by the J/3 electron detector on DMSP. The J/3 electron measurements were made on the same field lines as the X-ray sensor field of view and were averaged over a time interval that corresponds to the X-ray sensor field of view along the satellite ground track divided by the satellite velocity. Good agreement is evident; both the measured and inferred spectra indicate average electron energies of about 7 keV with a total energy flux of 10.8 ergs/cm^2-s.

The third panel in Figure 3 shows the ionization profile computed from the electron fluxes that were inferred from the X-ray data. For comparison we show the range in electron density measured by the radar in the auroral band at several different altitudes. At most altitudes the inferred densities are slightly less than the range in densities measured by the radar.

OBSERVATIONS OF A SUNLIT MORNING AURORA

On 15 June 1978 the DMSP satellite passed slightly to the east of Chatanika at 1546 UT (0546 local time on 16 June), as shown in Figure 4. Because this date is close to the summer solstice, sunrise at Chatanika was more than four hours prior to the DMSP pass. The solar zenith angle at Chatanika was about 70° during the satellite pass.

The Chatanika radar was operated in continuous sequential elevation scans for several hours before and after the satellite pass. Figure 5 shows the latitudinal distribution of ionization measured during the elevation scan made at the time of the satellite pass. A

broad region of diffuse aurora is visible over Chatanika with maximum ionization of about $3 \times 10^5 cm^{-3}$ between 115 and 120 km altitude. Thus, the average energy of the electrons producing the ionization was similar to that observed during the evening aurora described above. Because no visible auroral imagery was available for this sunlit case, we examined data from successive elevation scans to determine the stability of the auroral precipitation during the satellite pass. In Figure 6 we show the maximum E region electron density measured by the radar during nine consecutive elevation scans. The data are plotted as a function of invariant latitude and magnetic local time. The maximum E region densities were slightly higher at earlier local times, but the aurora was otherwise fairly stable. The locations of measurements made during the scan that was simultaneous with the DMSP satellite pass are shown by the heavy line on the left side of the plot. The DMSP trajectory and the X-ray detector field of view are also shown.

An X-ray spectral distribution measured by the DMSP instrument during the satellites passage over the diffuse aurora is shown in the first panel of Figure 7. Comparing this spectral distribution with that shown in Figure 3 shows that the spectral shapes are very similar, with the morning sector fluxes lower by about a factor of seven from those measured in the evening sector event. The inferred electron spectrum therefore has an average energy of about 6 keV and energy flux of 1.5 ergs/cm^2-s. The middle panel of Figure 7 shows the production rate of ionization resulting from the inferred electron fluxes. The peak ionization rate occurs near 115 km altitude and falls off rapidly at altitudes above the peak. However, solar illumination must also be taken into account in estimating the observed ionization. The rate of ionization produced by solar illumination for a solar zenith angle of 70° was determined using the results of Robinson and Vondrak (1984) and is shown in the middle panel of Figure 7. Although the ionization produced near the E region peak by sunlight is small compared to that produced by precipitating electrons, the solar contribution is dominant at higher altitudes. The resulting electron densities are shown in the third panel of Figure 7. For comparison, the horizontal bars show the range in electron densities measured by the radar across the diffuse auroral region. The inferred profile falls well within the range observed by the radar.

SUMMARY AND DISCUSSION

The comparative analysis of the Chatanika/DMSP data sets shows that satellite-borne X-ray measurements can be used to infer quantitatively the spatial distribution of electron energy deposition and ionization in the auroral ionosphere. For all the cases that were analyzed, the X-ray measurements could be used to identify the regions of electron energy distribution measured independently with the Chatanika radar and the all-sky camera. For two of the cases, auroral conditions were sufficiently uniform and stable to allow a detailed comparison between electron densities computed from inferred energetic electron fluxes and electron densities measured directly by incoherent scatter radar. The data were obtained during observations of an active evening sector aurora and a morning sector diffuse aurora. The average energy of the precipitating electrons in both cases was about 6 keV in the most intense regions. The energy flux in the morning sector event was lower by about a factor of seven from that in the evening sector event. This difference in the inferred energy flux was consistent with the factor of two to three difference in the E-region peak electron density. Because the morning sector aurora was sunlit, the contribution to the total ionization produced by photoionization had to be added to bring the inferred and measured profiles into agreement. This is the first time quantitative remote sensing of ionization in a sunlit aurora has been accomplished.

In the two cases described in detail above, the X-ray measurements represented spatial averages because of the large field of view of the detector. Thus, the inferred profiles were compared with the range in electron densities measured by the radar during a scan. The agreement between the inferred and measured densities depends on a combination of statistical accuracy of the measurements, temporal variations of the ionosphere, inhomogeneities over the satellite sensor field of view, and uncertainties in the calculation of ionization from the bremsstrahlung measurements. An additional uncertainty in the X-ray remote sensing technique is the presence of proton precipitation. Although electrons are the dominant source of ionization in the aurora on a global basis, precipitating protons can occasionally produce comparable or even greater amounts of ionization (*Basu et al.*, 1987). Because precipitating protons produce no bremsstrahlung X-rays, their presence and the associated ionization cannot be detected by the X-ray imager.

Despite these uncertainties, it is obvious from our results that the X-ray remote sensing technique holds great promise for monitoring auroral electron precipitation on a global

basis. Because the X-ray technique also yields information about the spectral distribution of the auroral electrons, these measurements can be used to determine the height profile of electron density at altitudes below 200 km. Further observations of the type described above are important in establishing the range in auroral conditions under which the technique is applicable.

REFERENCES

Baron, M. J., The Chatanika Radar System, in *Radar Probing of the Auroral Plasma*, Proceedings of the EISCAT Summer School, Tromso, Norway, June 5-13, 1975, A. Brekke, ed., pp. 385-405 (Universitetsforlaget, Tromso-Oslo-Bergen, 1977).

Basu, B., J. Jasperse, R. Robinson, R. Vondrak and D. Evans, Linear transport theory of auroral proton precipitation: A comparison with observations, *J. Geophys. Res.*, *92*, 5920, 1987.

Brown, J. C., The deduction of energy spectra of non-thermal electrons in flares from the observed dynamic spectra of hard X-ray bursts, *Solar Phys.*, *18*, 489, 1972.

Leadabrand, R. L., M. J. Baron, J. Petriceks and H. F. Bates, Chatanika, Alaska, auroral zone incoherent scatter facility, *Radio Science*, *7*, 747, 1972.

Mizera, P. F., J. G. Luhmann, W. A. Kolasinski, and J. B. Blake, Correlate observations of aurora' arcs, electrons, and X-rays form a DMSP satellite, *J. Geophys. Res.*, *83*, 5573, 1978.

Mizera, P. F. and D. J. Gorney, X-rays from the aurora, Proc. European Geophysical Society, Polar Aurora Symposium, Leeds, England, 1982.

Rees, M. H., Auroral ionization and excitation by incident energetic electrons, *Planet. Space Sci.*, *11*, 1209, 1963.

Robinson, R. M., and R. R. Vondrak, Measurements of E-region ionization and conductivity produced by solar illumination at high latitudes, *J. Geophys. Res.*, *89*, 3951, 1984.

Vickrey, J. F., R. R. Vondrak and S. J. Matthews, Energy deposition by precipitating particles and Joule dissipation in the auroral ionosphere, *J. Geophys. Res.*, *87*, 5184, 1982.

Vondrak, R. R., Incoherent-scatter radar measurements of electric field and plasma in the auroral ionosphere, in *High Latitude Space Plasma Physics*, B. Hultqvist and T. Hagfors, ed., Plenum Press, N.Y., p. 73-94, (1983).

Vondrak, R. R. and R. M. Robinson, Inference of high latitude ionization and conductivity from AE-C measurements of auroral electron fluxes, *J. Geophys. Res.*, *90*, 7505, 1985.

Vondrak, R. R., R. M. Robinson, P. F. Mizera, and D. J. Gorney, X-ray spectrophotometric remote sensing of auroral ionization, submitted to *Radio Science*, 1987.

FIGURE CAPTIONS

Figure 1. DMSP groundtrack over Alaska on 21 February 1979. The location of the bright auroral band at 0732 UT is shaded. Also shown are the E-region limits of the Chatanika radar elevation scan and the field of view of the DMSP X-ray sensor.

Figure 2. Contour plot of electron densities as a function of altitude and invariant latitude measured by the radar during a meridion scan on 21 February, 1979.

Figure 3. X-ray fluxes measured by DMSP, electron fluxes measured by J/3 detector and inferred from X-ray measurements and measured and inferred electron densities for evening sector auroral band.

Figure 4. DMSP groundtrack over Alaska on 15 June 1978. The DMSP X-ray detector field of view is shown along with the latitudinal extent of the morning sector diffuse aurora observed by the radar.

Figure 5. Contour plot of electron densities as a function of altitude and invariant latitude measured by the radar during a meridion scan on 21 February, 1979.

Figure 6. Variation of peak E-region density with latitude and magnetic local time as inferred from nine consecutive radar elevation scans.

Figure 7. X-ray fluxes measured by DMSP, height profile of ionization production rate due to kilovolt electrons and sunlight, and measured and inferred electron densities for the morning sector sunlit diffuse aurora.

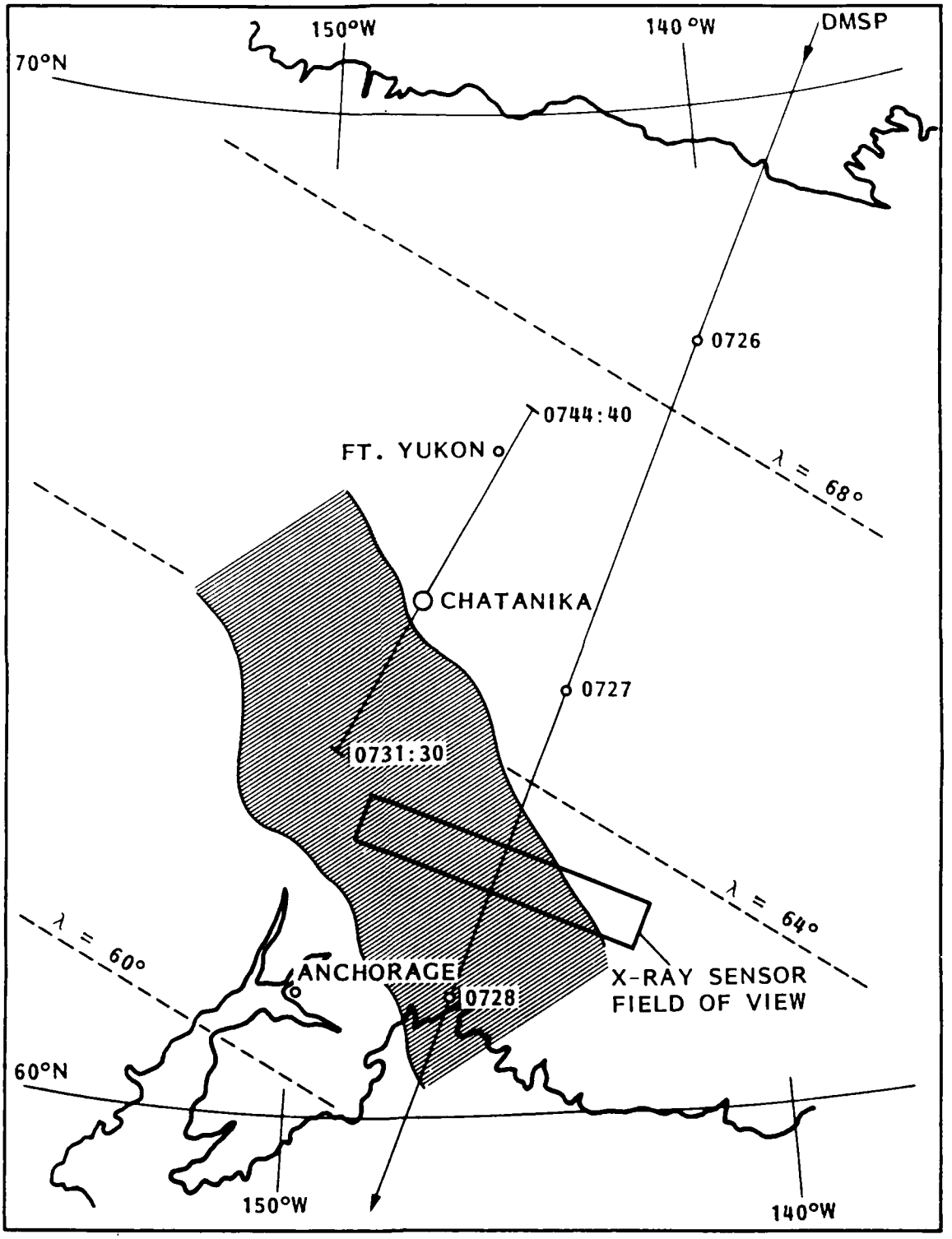
150°W
140 °W
DMSP
70°N
0726
0744:40
FT. YUKON
λ = 68°
CHATANIKA
0727
0731:30
λ = 64°
λ = 60°
ANCHORAGE
0728
X-RAY SENSOR
FIELD OF VIEW
60°N
150°W
140°W

FIGURE 1

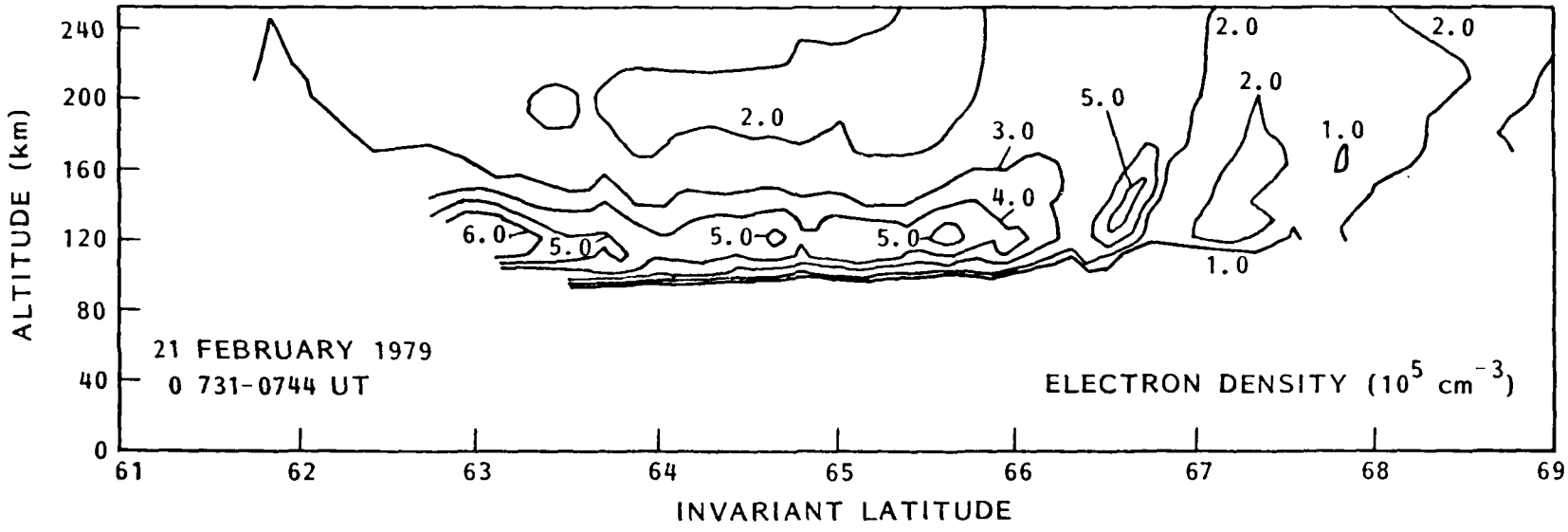
ALTITUDE (km)
240
200
160
120
80
40
0
61
62
63
64
65
66
67
68
69
INVARIANT LATITUDE
2.0
3.0
5.0
2.0
2.0
2.0
1.0
4.0
6.0
5.0
5.0
5.0
1.0
21 FEBRUARY 1979
0 731-0744 UT
ELECTRON DENSITY (10^5 cm^{-3})

FIGURE 2

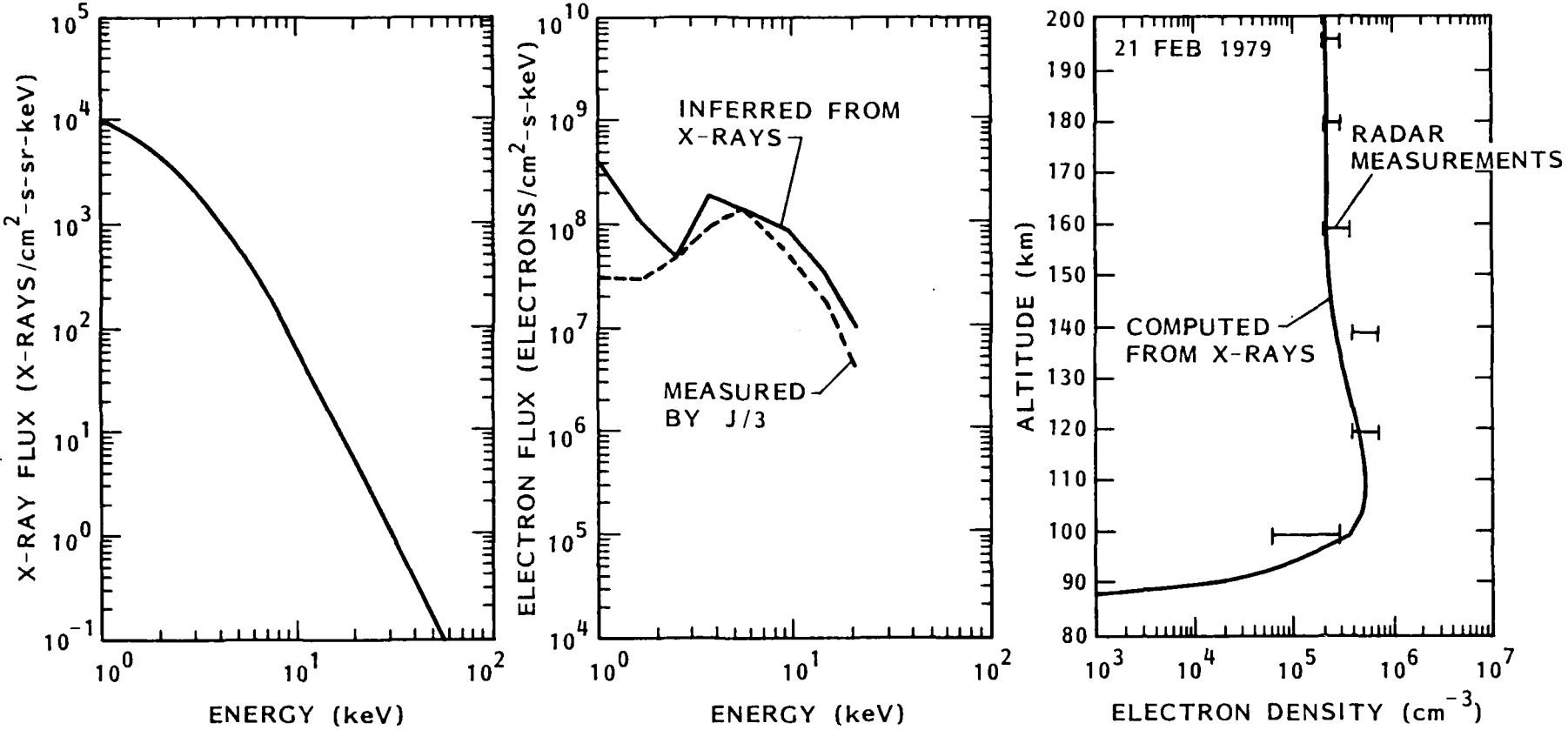
X-RAY FLUX (X-RAYS/cm^2-s-sr-keV)
ENERGY (keV)
ELECTRON FLUX (ELECTRONS/cm^2-s-keV)
INFERRED FROM X-RAYS
MEASURED BY J/3
ENERGY (keV)
21 FEB 1979
RADAR MEASUREMENTS
COMPUTED FROM X-RAYS
ALTITUDE (km)
ELECTRON DENSITY (cm^{-3})

FIGURE 3

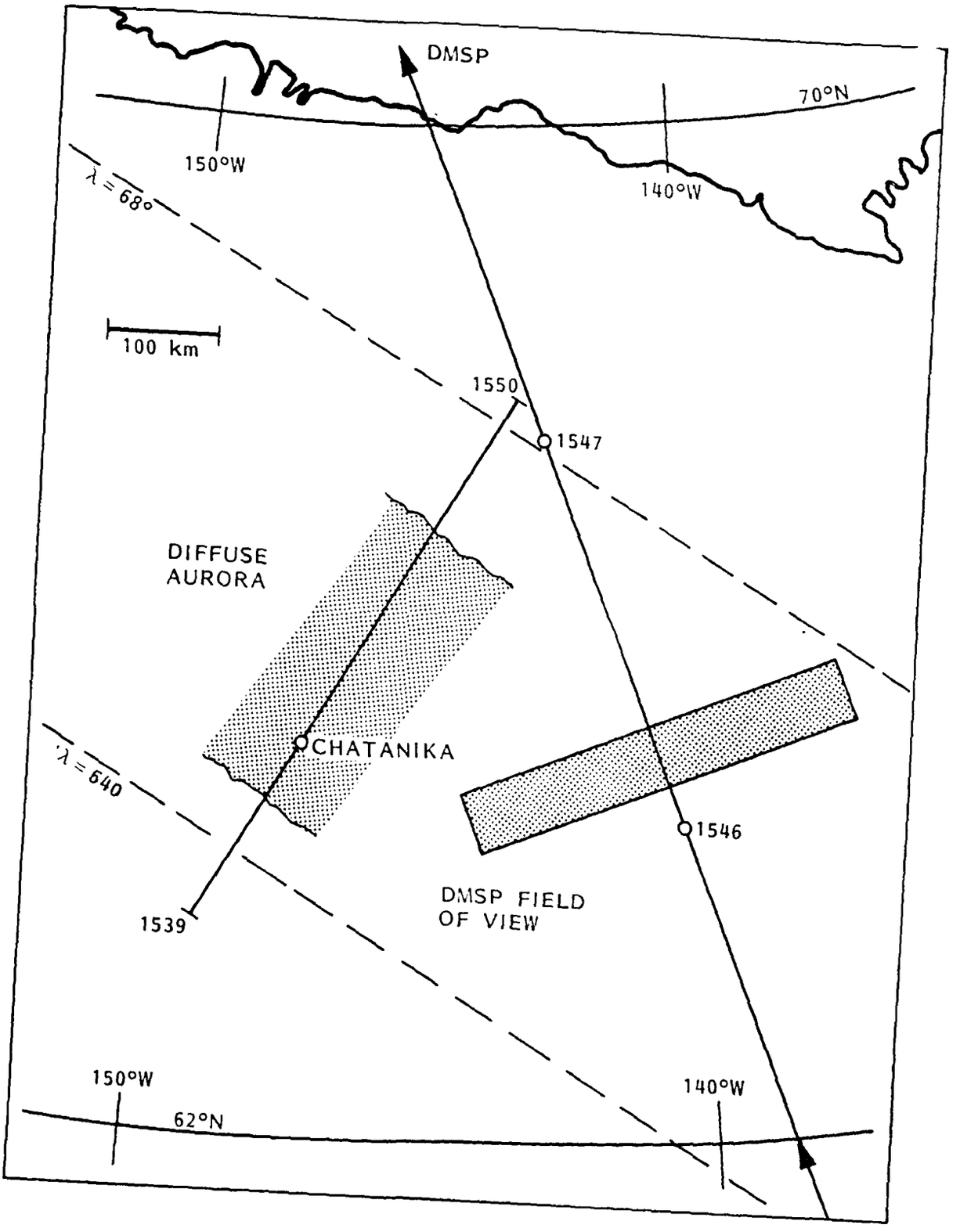
DMSP
70°N
150°W
140°W
λ = 68°
100 km
1550
1547
DIFFUSE
AURORA
CHATANIKA
λ = 64°
1546
1539
DMSP FIELD
OF VIEW
150°W
62°N
140°W

FIGURE 4

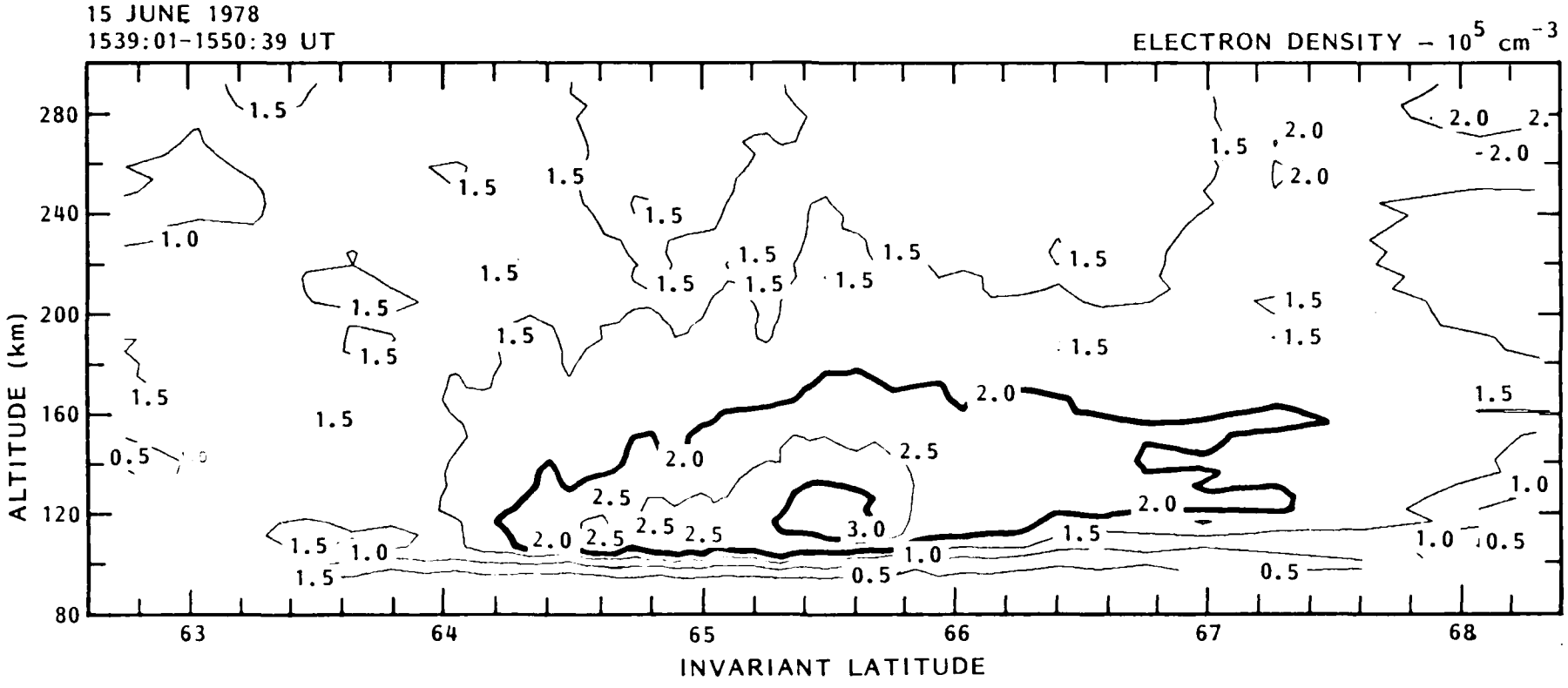
15 JUNE 1978
1539:01-1550:39 UT
ELECTRON DENSITY – 10^5 cm^{-3}
ALTITUDE (km)
INVARIANT LATITUDE
280
240
200
160
120
80
63
64
65
66
67
68

FIGURE 5

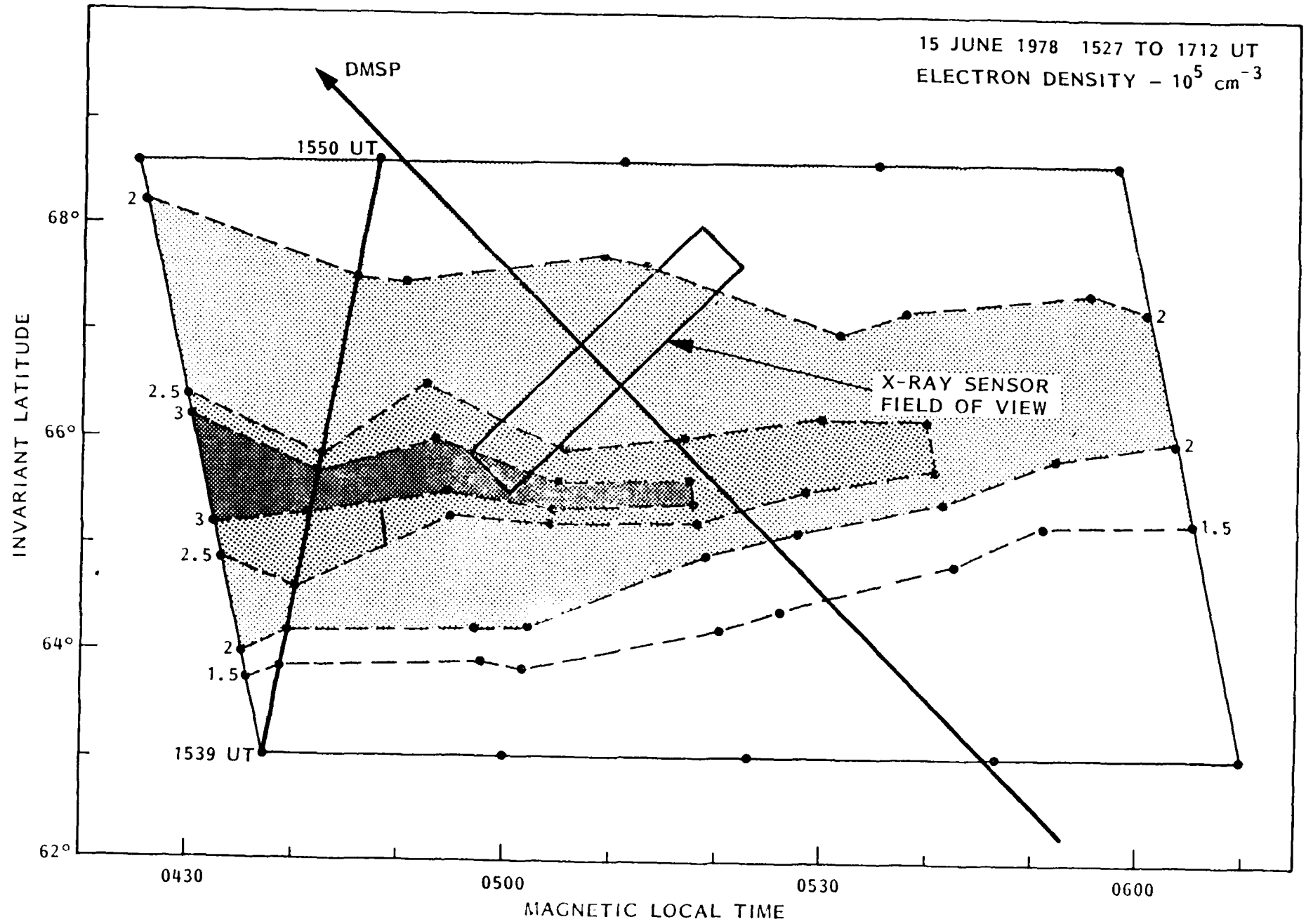
15 JUNE 1978 1527 TO 1712 UT
ELECTRON DENSITY – 10^5 cm^{-3}
DMSP
1550 UT
1539 UT
X-RAY SENSOR
FIELD OF VIEW
INVARIANT LATITUDE
68°
66°
64°
62°
0430
0500
0530
0600
MAGNETIC LOCAL TIME
2
2.5
3
3
2.5
2
1.5
2
2
1.5

FIGURE 6

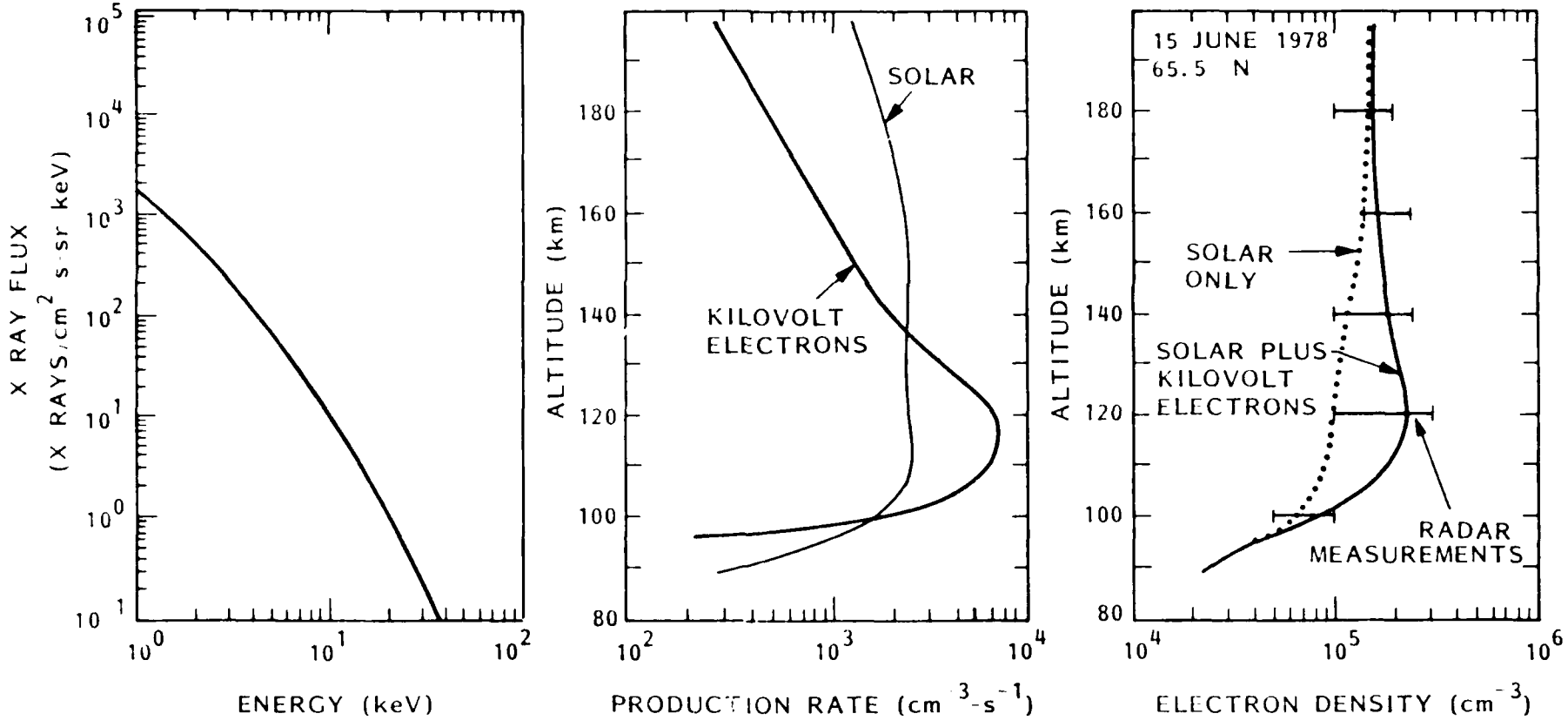
X RAY FLUX
(X RAYS/cm^2 s sr keV)
10^5
10^4
10^3
10^2
10^1
10^0
10^{-1}
10^0
10^1
10^2
ENERGY (keV)
ALTITUDE (km)
180
160
140
120
100
80
SOLAR
KILOVOLT
ELECTRONS
10^2
10^3
10^4
PRODUCTION RATE (cm^{-3}-s^{-1})
15 JUNE 1978
65.5 N
SOLAR
ONLY
SOLAR PLUS
KILOVOLT
ELECTRONS
RADAR
MEASUREMENTS
10^4
10^5
10^6
ELECTRON DENSITY (cm^{-3})

FIGURE 7

END
DATE
FILMD
3-88
DTIC

END
DATE
FILMD
3-88
DTIC